Environmental Modelling and Software 178 (2024) 106049

Contents lists available at ScienceDirect

Environmental Modelling and Software

journal homepage: www.elsevier.com/locate/envsoft

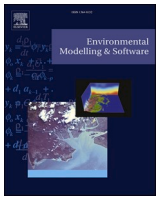

Coupling hydrological and sanitation datasets to simulate wastewater-derived contamination in European rivers: Model development and calibration

Janick Klink [a,b], Laura Aixalà Perelló [a,b], Morgan Abily [a,b], Joan Saló [a,b], Ignasi Rodríguez-Roda [a,c], Rafael Marcé [a,b,e], Wolfgang Gernjak [a,d], Lluís Corominas [a,b,*]

[a] Catalan Institute for Water Research (ICRA-CERCA), Emili Grahit 101, 17003, Girona, Spain
[b] University of Girona, Plaça de Sant Domènec, 3, 17004, Girona, Spain
[c] Laboratory of Chemical and Environmental Engineering (LEQUiA), Institute of the Environment, University of Girona, 17071, Girona, Spain
[d] Catalan Institution for Research and Advanced Studies (ICREA), Passeig Lluís Companys 23, 08010, Barcelona, Spain
[e] Centre d'Estudis Avançats de Blanes (CEAB-CSIC), Accés a la Cala Sant Francesc 14, 17003, Blanes, Spain

ARTICLE INFO

Handling Editor: Daniel P Ames

Keywords:
Microcontaminants
Fate and transport model
Open-source data
Water quality
Graph
River basin

ABSTRACT

Wastewater treatment plant (WWTP) discharges of microcontaminants negatively impact freshwater streams, underscoring the need for accurately mapping wastewater-derived contamination in water bodies across Europe (EU). In this study, we present a fast and open-source code for a microcontaminants fate and transport (MFT) model, capable of simulating contamination at a high resolution (15 arc second scale) across the EU. The model was developed using the best publicly available hydrological (HydroSHEDS) and sanitation (UWWTD) datasets and was rigorously calibrated, with a goodness of fit of 77.5% as measured by the R^2. Importantly, the model demonstrated the ability to predict wastewater-derived contamination in water bodies, making it a valuable tool for planning the upgrade of WWTPs and improving the ecological condition of freshwater streams in the EU.

1. Introduction

Chemicals are a necessary component of our daily lives. The database REACH contains between 30 and 50 thousand of such industrial chemicals, each of which may potentially be discharged into water bodies (Schwarzenbach et al., 2006). Microcontaminants are chemicals present in low concentrations in water matrices, which can be harmful for ecosystems or human health. Microcontaminants include pharmaceuticals, endocrine disruptors, and personal care products. Sewers and Wastewater Treatment Plants (WWTPs) are designed to remove nitrogen, and phosphorus, but not microcontaminants. As a result, wastewater-derived contamination is one of the primary reasons that surface water bodies do not satisfy the requirements for good chemical status (Whalley et al., 2018). Over the last decades, legislators have taken action to reduce chemical pollution of water, mostly following the precautionary principle. Such laws include The Water Framework Directive (WFD) in Europe and the Clean Water Act (CWA) in the United States. (An Act to Amend the Federal Water Pollution Control Act, 1971; European Parliament and European Council, 2000). Despite these legislative efforts, many contaminants continue to reach the natural environment. The new European Union (EU) rules on surface and groundwater pollution recognize this and call for an urgent reduction in micro contamination (European Commission, 2022). Legislators could hypothetically ban or limit the use of all potentially harmful chemicals. Diclofenac, for example, was banned for agricultural use in India following adverse effects on vulture populations (Aldred, 2011). In practice, however, a full implementation of the precautionary principle is unfeasible, because the produced chemicals likely provide some health or economic benefit. In the absence of a blanket ban, reducing micro contamination through advanced wastewater treatment is key for improving chemical status of surface water bodies. Lowering chemical consumption may also help, but it does not eliminate the need for advanced treatment (Corominas et al., 2021).

Implementing advanced treatment at conventional WWTPs entails an initial infrastructure investment and an increase in operational costs. These costs are not only monetary, but also environmental through CO_2

* Corresponding author. Emili Grahit 101, 17003, Girona, Spain.
E-mail addresses: janick.klink@upf.edu (J. Klink), laixala@umh.es (L.A. Perelló), mabily@icra.cat (M. Abily), joansalograu@gmail.com (J. Saló), ignasi.rodriguezroda@udg.edu (I. Rodríguez-Roda), rmarce@icra.cat (R. Marcé), wgernjak@icra.cat (W. Gernjak), lcorominas@icra.cat (L. Corominas).

https://doi.org/10.1016/j.envsoft.2024.106049
Received 30 August 2023; Received in revised form 5 April 2024; Accepted 17 April 2024
Available online 26 April 2024

emissions (Corominas et al., 2020). Advanced wastewater treatment should therefore be implemented where wastewater contamination is most deleterious to surface water bodies. This is where the development of microcontaminant fate and transport (MFT) models can be beneficial. Such models can simulate contamination where no field data is available, they can identify hotspots of wastewater-derived contamination and they can evaluate counterfactual strategies to protect water body ecosystems and human health. As a result, researchers have developed many spatially distributed MFT models. These include models such as GREAT-ER (Koormann et al., 2006), iSTREEM (Kapo et al., 2016), LF2000-WQX (Young et al., 2003), PhATE (Cunningham et al., 2012), Gimeno et al. (2017) and others. The majority of these models have limited geographical scope and are sometimes limited to single basins. Nowadays, large-scale free digital hydrologic and wastewater sanitation layers are available, allowing MFT models to be developed at large hydrological scales (e.g. Font et al., 2019; Grill et al., 2018).

Historically, calibrating and validating the accuracy of large-scale models has been a challenging task due to inadequate observations, coarse resolution of models, or limited computing resources. As a result, the accuracy of spatial predictions of microcontaminant concentrations has been deemed imprecise, with modeling exercises often indicating orders-of-magnitude differences from observations. Calibrations or validations of most MFT models have been conducted by comparing the orders-of-magnitude of modelled concentrations or loads to observations or by examining the distributions of simulated and observed concentrations or loads. Hence the goal of this study is to develop a large-scale MFT model (wOtter) that can rapidly simulate wastewater-derived contamination at a large scale and fine resolution and calibrate it. To demonstrate the capabilities of the model, we implemented the model for water bodies in the European Union, Serbia, the United Kingdom, Switzerland, and Norway. This study focused on the impact of micro-contamination derived from household wastewater on water bodies under average conditions. The hydrological data derive from the HydroSHEDS dataset, while the Urban Wastewater Directive database (UWWTD) in combination with the Water Sanitation and Hygiene database (WASH) supplied information on wastewater and wastewater treatment. We calibrated the model against a lumped contaminant, which is as a weighted average of the concentrations of multiple contaminants. We believe that this index serves as a better proxy for overall river contamination.

2. Materials and methods

wOtter processes data on sanitation, rivers and lakes (dams and reservoirs are included as lakes). In the sanitation section, the data on WWTPs is transformed into a data frame (.csv file) containing information on the served population (in person equivalents), the treatment level (primary, secondary, or tertiary) and the point of entry of treated wastewater into the river. A vectorial representation of rivers is converted to a graph object in the rivers section, which contains information on discharges, residence times, as well as the topographical order of the nodes. If a part of the river is identified as a lake, reservoir or dam, residence times are replaced by a lake-specific residence time. In the graph section, the data on sanitation, rivers and lakes, dams and reservoirs come together. Contamination enters the river through discharge points, is propagated through the river networks, and is attenuated using residence times. The programming structure is shown in Fig. 1, and a detailed user manual is available in the supplementary material.

We discuss the data of the hydrological network, sanitation, and occurrences of contamination in rivers in Sect. 2.1. In Sect. 2.2 we provide a brief explanation of the river graph generation and the residence times calculation. Following this, we describe the method for calculating the contamination load entering the river network and the method for applying attenuation. Section 2.3 discusses the construction of the lumped contaminant. In Sect. 2.4, we present the model calibration methodology. Section 2.5 explains the contamination score, which is a way of representing the results.

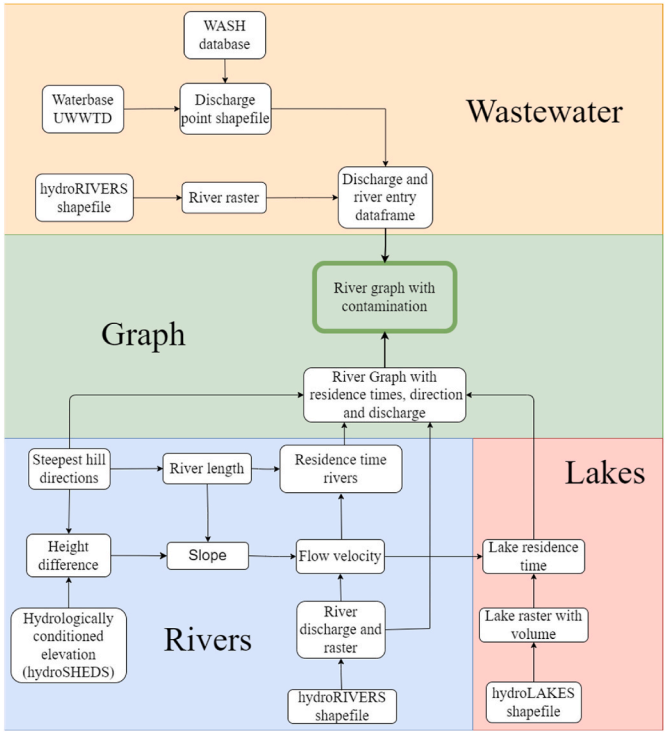

Fig. 1. The process flow of wOtter.

2.1. Data

This study encompasses the European Union member states, the United Kingdom, Switzerland, Serbia, and Norway. An online version of the model with a link to the input files is available at https://github.com/icra/wOtter.

2.1.1. Water bodies

The information on the river network derives from the HydroSHEDS database (Lehner et al., 2008). HydroSHEDS in turn uses waterGAP and satellite imagery to calculate river discharges (Alcamo et al., 2003). The resolution of river locations and discharges is 15″ (arc seconds), which corresponds to a maximum length and width of 450 m. The discharges are averaged over a year. Data on lakes, dams and reservoirs in Europe come from HydroSHEDS as well. This data includes the location of these water bodies and their volumes.

2.1.2. Sanitation

The two sources of sanitation data in Europe are the UWWTD database and the WASH database. The UWWTD database contains information on WWTPs in Europe that serve more than 2000 person equivalents (PE), and some smaller ones that voluntarily report to the database. All reported WWTPs have information on the load entering the plant in PE and the treatment levels available at the WWTP. We utilized the UWWTD database and addressed various errors encountered. The reconciled databases are available at this GitHub repository (https://github.com/icra/waterbase-uwwtd/tree/master/src/1-export_mdb_to_sqlite/db_versions), and a visualization of the corrected errors can be viewed at this link (https://waterbase.icradev.cat/). The WASH database provides national data on wastewater treatment or lack thereof. We use this data to create new sources of wastewater that are not included in the UWWTD database, such as untreated wastewater sources. We also use WASH to calculate correction factors for discrepancies between the PE found in a region according to the UWWTD database and the population with access to wastewater treatment according to the WASH database.

2.1.3. Microcontaminant occurrence dataset

We used the data on occurrences reported in Wilkinson et al. (2022) to calibrate and validate the model. The occurrence data included observations on 61 pharmaceuticals at 1052 sampling sites, 320 of which fell within the geographical scope of the study. We calibrated using 273 sampling sites, as 47 sites were removed for a variety of reasons after studying each site manually. We removed some sampling sites in Utrecht as anthropogenic changes to rivers made the river system too complex to be modelled by HydroRIVERS. We also removed any sample sites that, as reported by Wilkinson et al. (2022), were located in small ponds or urban drainages rather than rivers. Finally, we removed some sampling sites that measured sewage directly. Justification for each removal is provided in the supplementary material S2.

2.2. Model construction

2.2.1. Creation of the river graph

The creation of the river graph began with the HydroSHEDS database, which contains data on Europe's river network, (average) river discharges and flow directions. We converted the river network from a vectorial representation into a 15″ raster. At confluences, the highest among the two river discharges was chosen. A river graph was created from the raster by creating a graph node for each river cell. The position of the river cell in the raster became the node's unique identifier, such that the node could always be converted to a position in the raster or vice versa. This identifier based on the raster simplifies uploading geographical data, and was used to upload data on discharges, flow directions and lake presence to the river graph's nodes. The flow directions determined the topographical structure of the river graph, by forming directed edges from one river cell to the cell downstream.

We calculated the residence times RT [h] following the approach of Font et al. (2019). For rivers, the residence time was the length of a cell l [m] divided by the flow velocity v $[\mathrm{m\ h^{-1}}]$. For lakes, the residence time was calculated as the inverse proportion of outflow per hour, which required data on volumes Vol $[\mathrm{m^3}]$ and discharges q $[\mathrm{m^3\ h^{-1}}]$ unless otherwise specified).

$$RT = \frac{l}{v}\ (\text{rivers}). \tag{1}$$

$$RT = \frac{Vol}{q}\ (\text{lakes, dams and reservoirs}). \tag{2}$$

The length of a river node was determined by the cell size, which was in turn determined by the latitude. Cells are 450 m horizontally and range between 160 and 380 m vertically. If the river flowed horizontally or vertically, we stored the horizontal or vertical length; otherwise, we stored the diagonal length. We estimated the flow velocity using the hydraulic radius and then the Manning equation.

To calculate the hydraulic radius R $[m]$, we estimated the width w $[m]$ and height h $[m]$ of the riverbed. We used eqs. (3) and (4) from Allen et al. (1994), with discharge q in $[\mathrm{m^3\ s^{-1}}]$:

$$w = 2.71 * q\left[\mathrm{m^3 s^{-1}}\right]^{0.557}. \tag{3}$$

$$h = 0.349 * q\left[\mathrm{m^3 s^{-1}}\right]^{0.341}. \tag{4}$$

We calculated the hydraulic radius R $[m]$ following Schulze et al. (2005) with eq. (5). This equation is derived by assuming rectangular river beds.

$$R = \frac{wh}{2h + w}. \tag{5}$$

We also follow Schulze et al. (2005) in calculating the flow velocity v $[\mathrm{m\ h^{-1}}]$. In this equation, S is the slope $[\mathrm{m\ m^{-1}}]$, which we derive using elevation data from HydroSHEDS.

$$v\left[\mathrm{m\ s^{-1}}\right] = 22.7 \frac{\mathrm{m^{\frac{1}{3}}}}{\mathrm{s}}\ R^{\frac{2}{3}} S^{\frac{1}{2}}. \tag{6}$$

$$v\left[\mathrm{m\ h^{-1}}\right] = 3600\ \mathrm{s\ /\ h} * v\left[\mathrm{m\ s^{-1}}\right] \tag{7}$$

We obtain the residence time for each river cell by using this flow velocity and eq. (1).

2.2.2. Creation of the contamination discharge

2.2.2.1. Wastewater collection and treatment pathway. The UWWTD database contains data on WWTPs. It reports the treatment level at the plant as well as the influent in PE units. The influent includes the load from industry. Since this paper focuses on microcontaminants in household wastewater, we removed the portion of the load in PE units that enters WWTPs from industry. We estimated this portion using the WASH database, which contained data on the population that is connected to WWTPs by country. For example, if the WASH database estimated that 8 million people were connected to wastewater plants in a specific country, but the UWWTD database reported 10 million PE, then the load of each wastewater plant in that country was reduced by 20 percent. The approach is inspired by Vigiak et al. (2020).

We hence calculate a correction factor α_i $[persons\ PE^{-1}]$ that converts the PE load into persons for a WWTP in country i using eq. (8).

$$\alpha_i = \frac{people\ in\ country\ i\ connected\ to\ WWTPs\ according\ to\ WASH}{total\ reported\ PE\ of\ the\ WWTPs\ in\ country\ i\ according\ to\ UWWTD}. \tag{8}$$

And for a treatment plant j that is in country i, we obtain an estimated population for plant j using eq. (9)

$$Estimated\ population_j = \alpha_i * reported\ PE_j. \tag{9}$$

We require two additional parameters to calculate the contamination discharged from WWTPs into water bodies. The first is a wastewater treatment efficacy ϵ_{t_l} associated with treatment level t (primary, secondary, tertiary) at the WWTP l, and the second is the scale parameter γ, which accounts for the consumption of chemicals and their excretion in urine and feces after intake. We call γ a scale parameter because it determines the scale of the predictions of the model. γ is of the form $\mu g\ h^{-1}/person$. The treatment parameters ϵ_t are unitless.

The contamination load L_l $\left[\mu \mathrm{g\ h^{-1}}\right]$ coming from a WWTP indexed by l is then:

$$L_l = \gamma * Estimated\ Population_l * (1 - \epsilon_{t_l}) = \gamma * d_l. \tag{10}$$

With $d_l := Estimated\ Population_l * (1 - \epsilon_{t_l})$. We call d_l $[persons]$ the unscaled load since the scale parameter γ has not yet been applied.

2.2.2.2. Other pathways. The WASH database provides information on wastewater discharge to water bodies with pathways different from collection and treatment. It contains the number of inhabitants in each country that are not connected to WWTPs and the number of inhabitants with in situ wastewater treatment (individual appropriate systems, latrines; see: S5). These inhabitants and their associated contaminants loads were assigned to the least populated subbasins from HydroSHEDS (resolution level 7) in accordance with the total population of the basin. Because Serbia lacked wastewater treatment even in urban areas, raw discharges were assigned to urban areas. The contamination enters the water bodies through an artificial discharge point that is created at the location of a city, if such a city exist within the basin according to the UWWTD database. If the subbasin contained no cities, a discharge point was created randomly within the basin.

2.2.3. Contaminants routing

Contamination in a river node can come from upstream river nodes, or from a discharge point such as a WWTP if the river node is closest to the discharge point. The contamination entering the river node from the various sources is summed. Formally, let P_i denote the set of parent nodes of node i. These parent nodes are the upstream river cells, so there are none if the cell is the river's origin, one if it is a midsection and two if it is a confluence. Let D_i denote the set of wastewater discharges directly to node i. Typically, there are no direct discharges or only one, though there can be multiple. Let L be the load from a river cell or a discharged point, with index $j \in P_i$ if it is a river or index $l \in D_i$ if it is a discharge point. The formula for the contamination entering a river cell i is given by eq. (11).

$$\textit{contamination entering cell } i \textit{ per hour} = \sum_{j \in P_i} L_j + \sum_{l \in D_i} L_l = \sum_{j \in P_i} L_j + \gamma \sum_{l \in D_i} d_l \tag{11}$$

The last equality follows by substitution of L_l according to eq. (10).

First-order attenuation is applied to each river node according to its residence time. The attenuation rate is obtained through calibration. Let $k\ [\mathrm{h}^{-1}]$ denote the attenuation in water bodies and let RT_i denote the residence time of cell i in hours.

$$L_i = \left(\sum_{j \in P_i} L_j + \gamma \sum_{l \in D_i} d_l \right) \exp\{-RT_i k\}. \tag{12}$$

Letting q_i be the discharge $[\mathrm{m}^3\ \mathrm{h}^{-1}]$, derived from the HydroSHEDS dataset, we calculate the concentrations with eq. (13).

$$c_i = \frac{L_i}{q_i}. \tag{13}$$

Where c_i has dimension $[\mu \mathrm{g\ m}^{-3}]$, which is equivalent to $[\mathrm{ng\ l}^{-1}]$.

2.3. Creation of a lumped contaminant

For model validation, we construct a lumped contaminant as a sum of normalized concentrations of several contaminants. A lumped contaminant averages out differences in consumption across areas served by WWTPs and differences in treatment efficacies at WWTPs for the same compound. It also averages out observational error when sampling. The leftover variance of the lumped contaminant should thus better represent spatial variability in wastewater-derived contamination, resulting in better model adjustment as well as more accurate calibration of parameters. To calculate the lumped contaminant, we normalize each contaminant by dividing its concentration in each sampling point by the standard deviation of concentrations in all sampling points. Subsequently, we sum the normalized concentrations. The lumped contaminant is thus constructed according to eq. (14).

$$O_i = \sum_{j \in J} \frac{O_{i,j}}{\sigma_j}. \tag{14}$$

Where J is the set of contaminants included in the lumped contaminant, $O_{i,j}$ are the concentrations of individual contaminants at each location i, and σ_j is the standard deviation of each chemical across observations. Note that in normalizing the concentrations of the individual compounds, we do not subtract the mean. This step is omitted since it would yield negative observations, which the model cannot handle.

The lumped contaminant is modelled as a single contaminant (Sect. 2.2.2 and Sect. 2.2.3). There is, however, a difference in the units. Whereas for single contaminants the concentrations c_i are expressed in [ng /l], for the lumped contaminant these are in normalized nanograms per liter $\left[\mathrm{ng\ ng}^{-1}\ \mathrm{l}^{-1}\right]$. Attenuation is nonetheless applied using eq. (12), as with a single contaminant.

A selection of chemicals was made from the 61 pharmaceuticals and drugs reported in Wilkinson et al. (2022) to construct the lumped contaminant. This selection involved two steps. In the first step, only pharmaceuticals and drugs that were detected at more than 70 of the 320 sampling sites were kept. This was to avoid the measurement error of assigning values to non-detect samples and those samples with concentrations under the limit of quantification. The procedure left 21 out of 61 pharmaceuticals.

In the second step, pharmaceuticals and drugs such as Nicotine and Caffeine were removed because they did not correlate as well with wastewater. This is because while these compounds indicate the presence of wastewater, they do not correlate well with the degree of contamination, as different WWTPs may differ in removal efficacies (see section 4.1). To determine the correlation between the compounds and wastewater, we first calculated a lumped contaminant with the 21 compounds obtained in step one. For each compound, the percentual contribution to the lumped contaminant per site was calculated. This percentual contribution was correlated with 13 observations that were highly affected by wastewater with levels of contamination higher than 6 times the average. 14 out of 21 contaminants showed a positive correlation with those observations, meaning that they were relatively overrepresented in observations affected by wastewater. The lumped contaminant was the sum of these 14 contaminants, normalized by dividing them by their respective standard deviations. The chosen compounds were Atenolol, Citalopram, Codeine, Cotinine, Desvenlafaxine, Diltiazem, Fexofenadine, Lidocaine, Propranolol, Ranitidine, Sitagliptin, Sulfamethoxazole, Trimethoprim, Venlafaxine. The filter steps are further illustrated and explained in S1. This supplementary material also contains the observatios used for the calibration. More information, such as application and removal at WWTPs of the compounds can be found in S7.

2.4. Model calibration

We adjusted the scale of the loads entering water bodies (parameter γ) and the attenuation in water bodies (parameter k) to best fit the observed concentrations of the contaminants, calibrating a single parameter value for the extent of the model. The treatment parameters ϵ_t were not calibrated, and were set equal to the 'toxicity removal rates' found by Pistocchi et al. (2022). That study found a toxicity removal rate of 70% for secondary treatment. This toxicity removal rate was used for all specifications, including the specifications in which an individual contaminant was calibrated. The exact values of the treatment parameters do not affect the results significantly as 98% of wastewater discharge comes from WWTPs with secondary treatment and we adjust for scale.

Observations from 273 sampling sites in Wilkinson et al. (2022) were used. The fit to the data was measured by the R^2 metric. Let O_i be the occurrence for the (lumped) contaminant at site i and $\widehat{O}_i$ be the model prediction at site i. $\overline{O}$ is the mean value of all the occurrences. The R^2 is equal to eq. (15).

$$R^2 = 1 - \frac{\sum_i (\widehat{O}_i - O_i)^2}{\sum (O_i - \overline{O})^2} \tag{15}$$

The optimal value for the scale parameter γ was derived analytically (see, S6). Let $RT_{l,i}$ be the residence time $[h]$ between some discharge point l and some location i. Let, d_l be the contamination coming from a discharge point (in persons) and k the attenuation parameter in water bodies. q_i is the river discharge. The set A is the set of all observations for the contaminant. The sum for y_i is over D_i, which is the set of discharge points whose discharge ultimately ends up in cell i. The optimal value for the scale parameter γ is given by eq. (16).

$$\gamma = \frac{\sum_{n \in A} O_n y_n}{\sum_{m \in A} y_m^2}, \text{with } y_i := \frac{1}{q_i} \sum_{l \in D_i} d_l \exp\{-RT_{l,i} k\}. \quad (16)$$

Where y_i has dimension $[persons\ h\ m^{-3}]$. The scale parameter γ adjusts such that the predictions $\widehat{O}_i = \gamma y_i$ have the same dimension as the observations O_i. The formula $\widehat{O}_i = \gamma y_i$ may be derived by iterating the recursive eq (12). When calibrating a lumped contaminant, γ has dimension $\left[\mu g\ \mu g^{-1} h^{-1}\ /person\right]$.

We calculated the optimal value for attenuation in water bodies k numerically with the SciPy package (Virtanen et al., 2020). We adjusted the scale parameter γ during this calibration such that k and γ were simultaneously optimal. One of the implications of running a calibration with the attenuation parameter and the scale parameter is that structural biases in residence times, river discharges and wastewater discharges do not affect the model predictions. The parameters γ and k absorb those structural biases and leave model predictions unaffected (see, S6). This is useful if the goal is to predict contamination rather than to find unbiased estimates of parameters.

2.5. Representation of results

The raw output of the model has a resolution of 15″, which is too large to gain general insights into the chemical state of a basin, or the state of rivers in a country. For this reason, the raw data needs to be aggregated such that we can assign a comparable contamination score to (geographical) areas, even if they are diverse in area size, in river discharge or in the extent that is covered by rivers. For instance, the score may compare countries as diverse as Germany and Spain, or basins as diverse as the Rhine (Switzerland) and the Manzanares (Spain). Hence, we constructed an aggregated measure of contamination for an area j that contains at least one river cell indexed by i. We call this aggregated measure of contamination the (contamination) score. The main parameters of the score are p and a, which determine the extent to which we allow cleaner rivers to compensate for more contaminated rivers, and the extent to which we weigh river cells with larger discharge. If p is large, then the score is higher if one river is highly contaminated and the other is not, as opposed to when both rivers are moderately contaminated. If q is large, then if a small river is heavily contaminated but the larger river is not, the score remains small, since the larger river has larger weight.

The first step in calculating the contamination score is to take the concentrations of a contaminant predicted by the model (our results use the lumped contaminant) and to exponentiate it with a free parameter p. If we set p larger than 1, then the contamination score increases faster than the contamination. If we set p smaller than 1, the score grows less than linearly. Large values for p hence punish unequal distributions of contamination, whereas smaller values for p result in a smaller score when contamination is homogeneous across water bodies. The score is given by eq. (17).

$$s_i = c_i^p. \quad (17)$$

The cells are weighted by cell discharge q_i. This weight is exponentiated by a. For larger values of a, rivers with more discharge have a larger weight in the aggregated value than do rivers with little discharge. If the value of a is 0, then all rivers are weighted equally. If the value for a is equal to p, then rivers are weighted such that the score is entirely determined by contamination loads, not by concentrations. The formula to determine the weight of a river cell is given by (18). The weight also increases linearly by length of the cell.

$$w_i = \beta_j * q_i^a * cell\ length_i. \quad (18)$$

The parameter $\beta_j = \frac{1}{\sum_{i\ in\ j} q_i^a * cell\ length_i}$ normalizes the weights such that the sum of weights in an area j is equal to 1. This ensures that areas with more rivers or larger river discharges do not, ceteris paribus, have larger scores. Note that the sum is over all the river cells i that are geographically located in area j.

The score of an area j in the set of areas J is given by eq. (19).

$$S_j = \delta \sum_{i\ in\ j} w_i s_i. \quad (19)$$

The parameter $\delta = \frac{|J|}{\sum_{j \in J} \sum_{i\ in\ j} w_i s_i}$ normalizes the score such that the average of the measure is 1. In the formula $|J|$ is the number of areas.

Score under results was shown for $p = 1.2$ and $a = 0.5$. We chose these values to punish areas that exhibit unequal distributions of contamination and to weigh river cells with much discharge more heavily than smaller those cells with smaller discharge. The score can be calculated quickly for other values of p and a, and there is no single correct combination of parameter values. We do not find large differences in the results when applying different p and a (results not shown). To conclude the materials and methods section we provide in Table 1 a summary of important parameters and variables used in wOtter.

3. Results

3.1. Goodness of model fit

The model adjustment of the calibrations is shown in Fig. 2. The calibration gives an adjustment for the R^2 of 77.5% (Fig. 2 (a)). While the graph shows logarithmic values for visibility, we used absolute values for calculating the R^2 and for the model calibration. The model performed better for smaller rivers than for larger rivers, with adjustments of 79% (Fig. 2 (c)) and 72% (Fig. 2 (b)) respectively. This is likely since smaller rivers often receive no wastewater discharge both in the model and in reality, such that the model accurately predicts the contamination level. The optimal attenuation rate for the lumped contaminant was 0.005 h^{-1}. With an attenuation of 0.005 h^{-1}, the total

Table 1
Selection of important parameters and variables used in wOtter. Dimension is included in the value column if the variable is not dimensionless.

Variable/ parameter	Source	Value	Purpose
Discharge q_i	HydroSheds	River i dependent [$m^3 h^{-1}$]	Determines dilution
Residence time RT_i	Own calculations using HydroSheds data	River i dependent [h]	Determines compound attenuation
Treatment efficacy ϵ_t	Pistocchi et al. (2022)	Treatment t dependent 0, 0.33, 0.70, 0.92 (none, primary, secondary, tertiary)	Account for role of wastewater treatment.
Unscaled load d_l	Own calculations using UWWTD and WASH	Treatment plant l dependent [persons]	Determines wastewater load for rivers
Scale parameter γ	Calibration	Dependent on application to compound	Rescale model predictions to observations
Attenuation k	Calibration	Dependent on application to compound $\left[h^{-1}\right]$	Determines the compound attenuation per hour of residence time
Concentration c_i	Model output	River i dependent [$\mu g/l$] [$\mu g * \mu g^{-1}/l$ for lumped contaminants]	Estimates degree of contamination in river

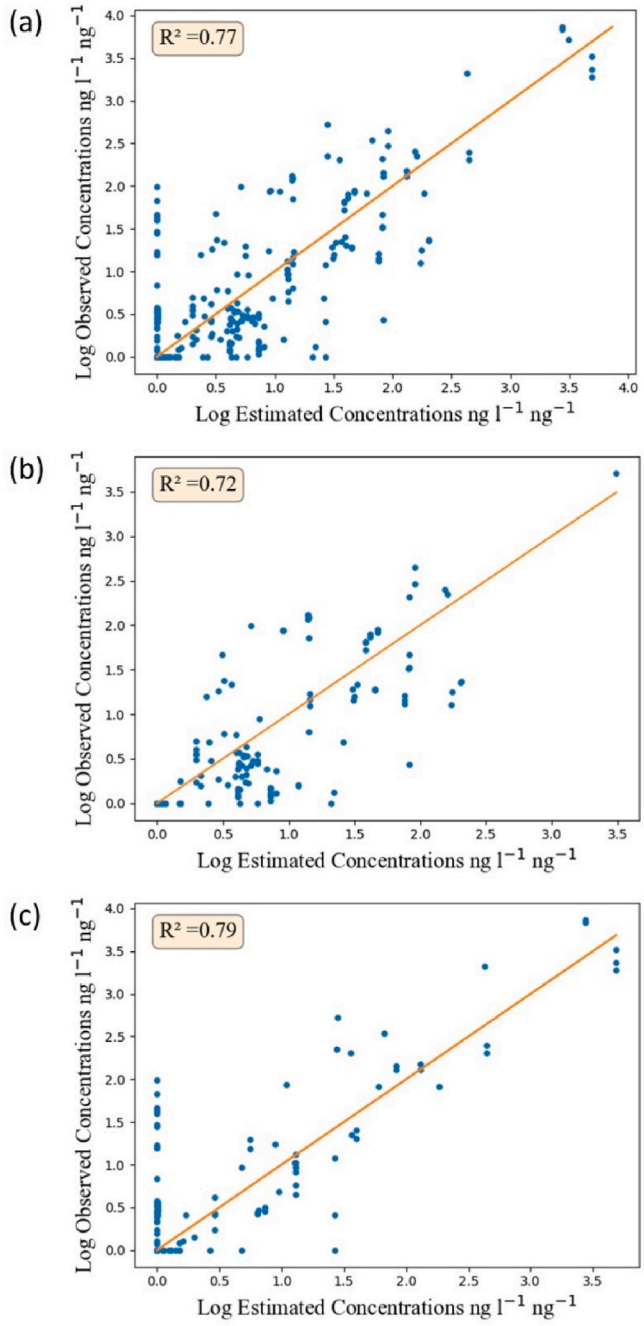

Fig. 2. WOtter model fit using the lumped contaminant. (a) using observations from 273 sampling sites, (b) using observations from sampling sites with discharge higher than median sampling site discharge of 10.4 $\mathbf{m^3\ s^{-1}}$ (bigger rivers), (c) using observations from sampling sites with discharge lower than median sampling site discharge of $\mathbf{10.4\ m^3\ s^{-1}}$ (smaller rivers). Observations concentrations are logarithmic only for visualization.

load of contamination entering oceans in the model is 38% lower than when no attenuation is assumed.

We compare the goodness of model fit obtained with the lumped contaminant of 14 pharmaceuticals to the average goodness of fit obtained from the individual calibration of 21 contaminants (obtained in step one of contaminants selection, Sect. 2.3), as well as to the lumped contaminants of 61 and 21 obtained in step one. The model fit using the lumped contaminant of 14 pharmaceuticals (77.5%) was much better than the average fit for individual contaminants (−3.5%). The negative average R^2 for the individual contaminants means that one could more accurately estimate contamination levels using only the mean. This shows the model is poor at predicting individual contaminant levels (see section 4.1). Among the alternatives of lumped contaminants, the one with 14 pharmaceuticals provided the best model fit (77.5%). The model attained an R^2 of 56.2% when predicting the lumped contaminant of 61. Since the lumped contaminant of 61 included all contaminants reported in Wilkinson et al. (2022), it permits no data dredging.

Calibration for the attenuation rates did not always result in acceptable estimates for the parameters. Predictions for the lumped contaminants of 21 and 61 best fit the data when the attenuation rate in water bodies was negative. For 19 out of the 21 individual contaminants, optimal attenuation rates were also found to be negative. In these cases, attenuation rates were set to 0 h^{-1}. Such unreasonable estimates of the attenuation rate are likely due to insufficient observations and lack of explanatory power of the attenuation parameter.

Table 2 reports the results of the different lumped calibrations. In addition to the R^2 and the attenuation parameter k, it also shows the scale parameter γ. The scale parameter γ does not have a physical interpretation for the normalized contaminants. Table 3 shows the same calibration results for the individual contaminants in the lumped contaminant of 21.

3.2. Model simulation

The predicted (normalized) concentrations of the lumped contaminant can range from zero to infinity. The value zero indicates that there is no wastewater discharge into the river. For rivers with discharge smaller than two cubic meters per second, we find that 79.4% of the rivers receive no wastewater (percentage of length). For rivers with discharges larger than 2 $m^3\ s^{-1}$, 44.7% of rivers are found to be uncontaminated. The Lorenz curve in Fig. 3 shows that river contamination is unequal, with 10% of river sections (corresponding to around 120,000 km assuming equal discharges) contributing to 50% of the sum of concentrations. The Gini index is equal to twice the area between the diagonal and the Lorenze curve. The Gini index is therefore 1 if only a single river section is contaminated and is 0 if all rivers are equally contaminated The resulting Gini index of 0.77 suggests contamination is very unequally distributed.

In the supporting material S3, we provide an interactive figure as an html file to visualize (normalized) concentrations of the lumped contaminant in European river streams. It contains the discharge points as well as the sample observations and model predictions. By zooming into the interactive figure in the supplement, one can see the degree of contamination in rivers, the contamination effect of wastewater discharges, and the accuracy of the model in predicting specific sample observations. Fig. 4 is a snapshot of S3 that depicts wastewater-derived contamination in central and southern Europe. Fig. 5 shows snapshots of the map limited to a wastewater treatment plant in Madrid, with a visualization of the available data for rivers, observations, and discharge points.

Fig. 6 shows that the basins most contaminated by wastewater are in Holland and Flevoland (Netherlands), Murcia (Spain) and Vojvodina (Serbia). The contamination score for these basins is more than eight times larger than the standardized score of 1. The causes of

Table 2
Goodness of fit and calibrated parameter values using different lumped contaminants. The $\mathbf{R^2}$ is a measure of goodness of fit and is calculated by eq. (15). The scale parameter $\boldsymbol{\gamma}$ adjusts the scale of the model to that of the observations and is given by eq. (16). The attenuation parameter $\boldsymbol{k}$ determines the attenuation in rivers (see eq. (12)).

	R^2	$\gamma\ (\mu g\ \mu g^{-1}\ h^{-1}\ /person)$	$k\ (h^{-1})$
Lumped 14	77.5%	1.88	0.46%
Lumped 21	58.1%	2.32	0.00%
Lumped 61	56.2%	3.47	0.00%

Table 3
Goodness of fit and calibrated parameter values for the individual contaminants included in the lumped contaminant of 21. The first entry in the table contains the average $\mathbf{R^2}$, γ and k of the entries below. The $\mathbf{R^2}$ is a measure of goodness of fit and is calculated by eq. (15). The scale parameter γ adjusts the scale of the model to that of the observations and is given by eq. (16). The attenuation parameter $\boldsymbol{k}$ determines the attenuation in rivers (see eq (12)).

	R^2	$\gamma\ \left(\mu g\, h^{-1}\, /person\right)$	$k\ \left(h^{-1}\right)$
Average of 21 individual calibrations	−3.5%	21.91	0.00%
Atenolol	0.5%	1.88	0.00%
Carbamazepine	−0.2%	2.32	0.04%
Caffeine	−21.1%	3.47	0.00%
Cetirizine	−2.9%	12.19	0.00%
Citalopram	−0.7%	30.47	0.00%
Codeine	−2.1%	56.46	0.00%
Cotinine	−2.9%	14.96	0.00%
Desvenlafaxine	−2.4%	2.71	0.00%
Diltiazem	−0.3%	6.99	0.00%
Fexofenadine	−8.6%	2.78	0.00%
Gabapentin	−0.7%	29.59	0.00%
Lidocaine	−3.2%	1.90	0.00%
Metformin	−16.3%	8.33	0.00%
Nicotine	−6.3%	107.00	0.00%
Paracetamol	−5.3%	3.22	0.00%
Propranolol	4.3%	156.44	0.08%
Ranitidine	−0.2%	5.20	0.00%
Sitagliptin	1.1%	22.57	0.00%
Sulfamethoxazole	−0.2%	4.70	0.00%
Trimethoprim	−2.3%	10.04	0.00%
Venlafaxine	−3.9%	28.15	0.00%

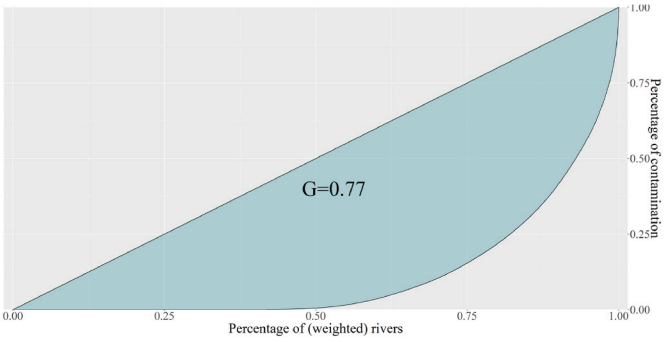

Fig. 3. Lorenz cure and Gini index of river contamination in European river sections. Percentage of rivers is determined according to weights. The weight of each river cell is equal to the distance it covers times the square root of the flow discharge.

contamination in these basins are diverse. According to the model, contamination in the Netherlands is primarily caused by large populations within the country, with only a minor contribution from large populations upstream in Germany. Water scarcity is the primary cause of high contamination levels in the Murcia basin. However, the model does not consider that most wastewater is recycled in Murcia for agriculture (esamur, 2022). As a result, contamination levels in Murcia are likely overestimated. Vojvodina (Serbia) is contaminated primarily due to a lack of sanitation in Serbia. WASH estimates that 42% of waste enters rivers untreated for Serbia.

Table 4 summarizes results on wastewater-derived contamination for all countries included in the study. The data shows that for some countries, contamination is a local problem whereas for others it is widespread. The Gini index is relatively low in the Netherlands and Hungary, indicating that contamination is spread evenly. The Gini index is much higher for countries such as Spain or Cyprus. This implies that only a few river sections are highly contaminated. As a result, efforts to reduce contamination in those countries should target a few hot spots.

The findings from this study can be compared to those of hydroWASTE (Ehalt MacEdo et al., 2022). We consistently find that more rivers receive wastewater-derived contamination when compared to hydroWASTE. We find between 1.2 and 1.8 times more length of rivers affected by wastewater in 23 of 31 countries. Other countries, such as Sweden, Norway, and Iceland, have even higher ratios. This is likely because some WWTPs in inner, sparsely populated regions are not reported or included in hydroWASTE, whereas our model includes an artificial discharge point for those areas.

3.3. Model functionality

The code and the model are available on GitHub as wOtter (https://github.com/icra/wOtter). We extensively commented all scripts, allowing any potential user to both understand our approach, and adapt it to any other goal. We used the NetworkX package to represent the river network as a graph object. This package enables users to store information within each river node, such as the country in which the node is located, the river node's ecological status or whether the node is part of a lake. In addition, the Networkx package includes a useful library, with functions that generate a topological sort of the river network or split the river network into basins.

We have also published a library with the model that provides useful operations. This library included functions to cut the river network by a geographical area or to find the closest river to a point in a shapefile. The library additionally contains functions for pre and post processing (Table 5).

The runtime of an individual simulation for the entire domain of European rivers is around 25 s on a standard laptop (Dell Latitude 5420). This runtime per individual simulation can be reduced if the user needs to implement many simulations, for instance when doing Monte-Carlo analysis. For such computationally intensive purposes, we have prepared a matrix-based implementation (see, S6) that simulates the model catchment-wise. The catchment is determined by the connectedness of the river cells. This implementation can complete a simulation for the Danube basin in 0.8 s.

4. Discussion

4.1. Use of the lumped contaminant

Our results show that wOtter predicts lumped contaminants better than it predicts any single contaminant. The model attains an R^2 of 77.5% when predicting the lumped contaminant of 14, whereas the best predicted contaminant, propranolol, is only predicted with an R^2 of 4.3%. Such accuracy in predicting individual contaminants is not untypical for the literature, which often does not report the R^2 but rather focuses on differences in distributions or magnitudes (Pistocchi et al., 2010, see section 4.2).

The lumped contaminant was better predicted by wOtter because it is a more reliable indicator for contamination by wastewater than any single substance (Kahle et al., 2009). This reliability is a consequence of filtering those compounds that best correlate with wastewater and a consequence of averaging out fluctuations in the occurrence of individual compounds. As such, observed concentrations for the lumped contaminant are less affected by (1) differential removal rates in wastewater treatment, (2) differential consumption patterns and (3) diffuse sourcing.

First, differential removal rates may result in magnitude differences in the concentrations of individual compounds (Verlicchi et al., 2012). Elimination ranges for Caffeine, for instance, may range from 81 to 99.9% (Buerge et al., 2003). This implies that Caffeine may be found in concentrations up to 190 times larger in effluent depending on the treatment plant, even if both have secondary treatment. Caffeine may then still be a biomarker for wastewater if it is the predominant source of environmental entry, but it is hence a poor marker for the degree of

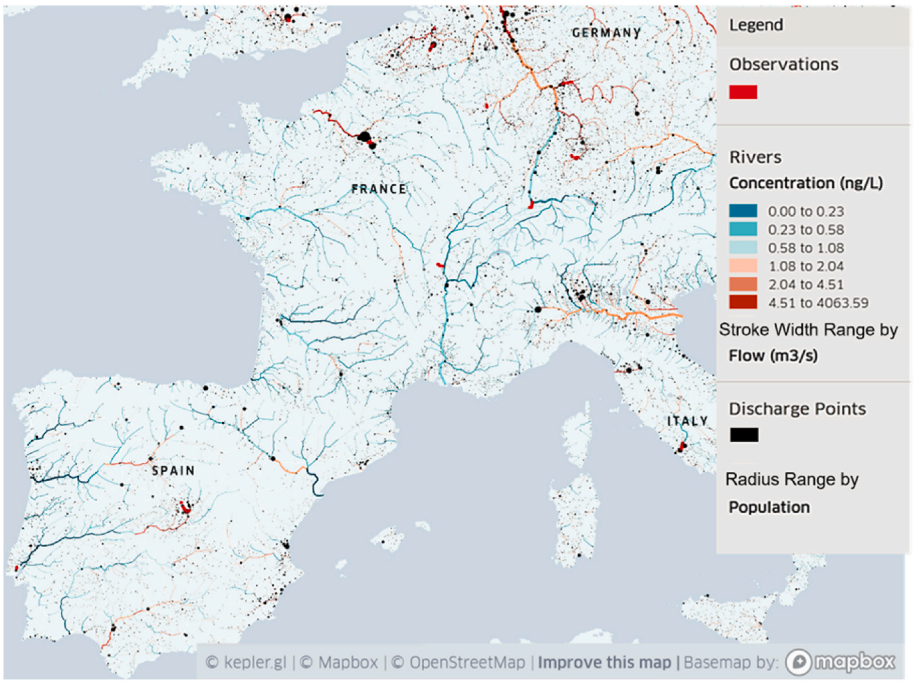

Fig. 4. An exported image of the interactive map in S3. The discharge is illustrated by the thickness of the river line and the contamination is given by the color. Reddish hues imply more contaminated rivers. The circles are wastewater discharge points that cause contamination in the rivers.

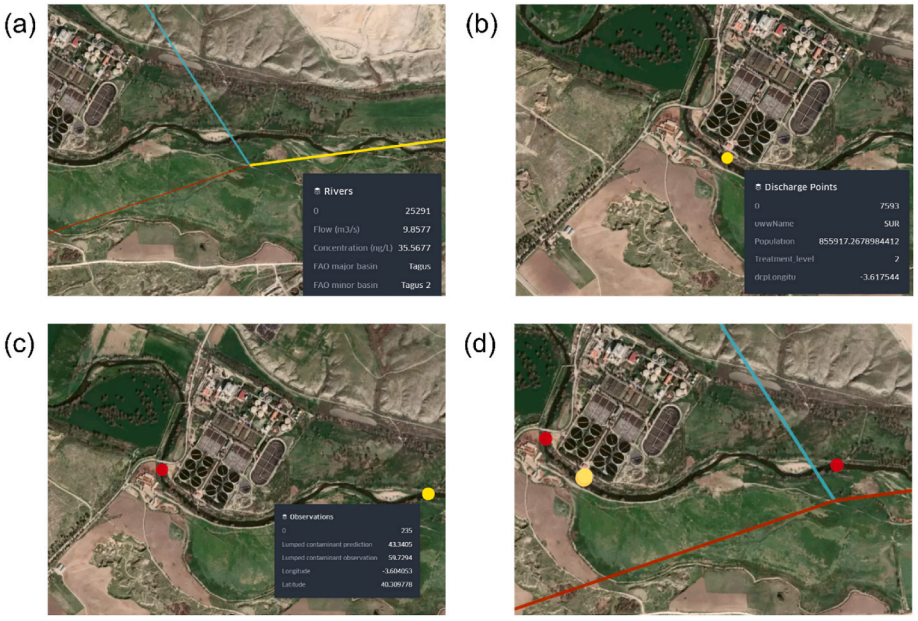

Fig. 5. The figure shows the wastewater plant EDAR SUR in Madrid Spain. The images are snapshots from the interactive figure from Kelper. gl in S3 Figure (a) shows the data fields for river sections, this includes the contamination. Figure (b) shows the discharge points, which have information on the treatment levels and the populations. Figure (c) shows the observations from Wilkinson et al. (2022) that are used for the model calibration. Figure (d) shows that the three datasets can be displayed simultaneously.

wastewater contamination. Second, some countries use or prescribe some compounds more commonly (e.g., Diener et al., 2008; Hoffman et al., 2019; Reyes and Cornelis, 2018). Gabapentin, for instance, differs by a magnitude of eight between Sweden and Switzerland in 2018 (Chan et al., 2023). Such discrepancies in use can be corrected for, but this requires reliable data on general use. Third, diffuse sources such as inappropriate disposal, urban runoff or illegal dumping may heavily affect the prevalence of a single compound in a single water sample. For instance, Nicotine may enter rivers through disposal of cigarette stubs. Diffuse sourcing may be especially relevant for Caffeine and Nicotine, as they are effectively removed by WWTPs. The results from Buerge et al. (2008), for instance, show that more than 30 percent of Nicotine does not derive from treated wastewater, and the author suggests that these may derive from raw wastewater through sewer overflows.

The occurrence of the lumped contaminant is not only easier to predict, but also more relevant due to being a reliable marker of wastewater contamination. Even when authors have used single compounds in validation, their presence is often argued to be important not

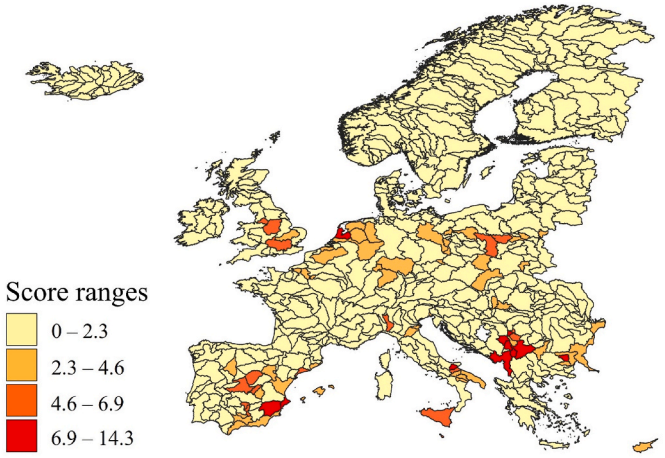

Fig. 6. Contamination per sub-basin. Sub-basins are taken from hydroSHEDS, who derive them with the Pfafstetter algorithm. Red hues signify more contaminated basins. The parameters of the measure are such that inequality in contamination is penalized, with p = 1.2 and a = 0.5 (see sec. 2.5). The score generally has no physically interpretable unit, and is unitless after normalization. An interactive version of Fig. 6 can be found in S4.

individually, but as a marker for wastewater contamination (e.g., Acuña et al., 2015a; Grill et al., 2018). Acuña et al. (2020) studies diclofenac because the study argues that it is a 'model' compound for the typical pharmaceutical. Anderson et al. (2004) corroborates the model Phate with what it calls 'surrogate compounds' that are meant to correlate with a more general conception of pharmaceutical contamination. Authors such as Abily et al. (2022), Rice and Westerhoff (2015) and Ehalt MacEdo et al. (2022) forego studying one contaminant and instead directly identify contamination with wastewater by using dilution factors.

4.2. Comparison against existing models

The high R^2 of 77.5% obtained in this study is, to our knowledge, the largest reported in the literature for MFT models. It improves on a study by Lämmchen et al. (2021) that obtained an R^2 of 57% when predicting median Metformin concentrations. However, that study separated occurrence data into those taken in summers and winters. They also introduced contamination from outside the model by performing a regression with intercept. Nevertheless, our goodness of fit and that of Lämmchen et al. (2021) are significant achievements, as many studies in this field do not report an R^2, and instead rely on other methods of validation (Pistocchi et al., 2010). For example, Anderson et al. (2004), Font et al. (2019), Grill et al. (2018), and Duarte et al. (2022) compare magnitude differences between observations and model predictions, while Kapo et al. (2016), and Lämmchen et al. (2021) validate their studies by comparing distributions of observations and model predictions. Such methods of validation are widely accepted because in many cases MFT models are not accurate enough to use the R^2 as a metric of fit.

Our results suggest that MFT models can accurately predict wastewater contamination, but have had low to medium performance precisely because individual contaminants are poor indicators of wastewater contamination. Since wOtter predicts the lumped contaminant accurately, MFT models with similar methodology such as iStreem, GREAT-ER, hydroROUT and globalFATE should too. Anderson et al. (2004) and Grill et al. (2018) find a much lower goodness of fit despite methodological similarity. We hypothesize that this is mostly because the surrogate compound used in these studies (caffeine and estrogen respectively, among others) does not correlate well with overall wastewater contamination.

Table 4
Summary of contamination score, Gini indices and length of contaminated rivers in European water bodies. The column ratio gives the kilometers affected by our model over the kilometers affected by wastewater according to HydroWASTE.

Count	Score	Gini (%)	0 (km)	0 (%)	0-2 (km)	0-2 (%)	>2 (km)	>2 (%)	wOtter (km)	Hydro-WASTE (km)	Ratio
NLD	3.30	43	4621	56	1118	14	2522	31	3639	2892	1.26
SRB	3.20	75	17373	85	1782	9	1297	6	3078	2100	1.47
CYP	3.06	90	1572	86	101	6	152	8	253	192	1.32
BEL	2.66	61	3961	52	2075	27	1522	20	3596	2235	1.61
LUX	2.00	63	298	45	243	37	120	18	363	246	1.47
DEU	1.96	50	48740	57	22442	26	14110	17	36552	28206	1.30
POL	1.58	62	43148	61	20598	29	6925	10	27522	20539	1.34
BGR	1.54	68	18930	75	2613	10	3720	15	6334	3536	1.79
HUN	1.52	47	9968	46	6794	31	5062	23	11856	7731	1.53
SVK	1.51	64	7630	65	3028	26	1101	9	4129	3015	1.37
ITA	1.45	69	44854	60	20486	27	9630	13	30117	19177	1.57
ESP	1.30	81	83591	72	20193	17	12182	11	32375	22858	1.42
CZE	1.29	57	10479	58	5571	31	2047	11	7618	5641	1.35
GBR	1.19	85	52050	77	10641	16	4586	7	15227	10358	1.47
ROU	0.69	53	30754	54	24085	42	1908	3	25993	11458	2.27
HRV	0.57	57	9478	73	2740	21	838	6	3578	1145	3.12
FRA	0.56	64	92800	68	39183	29	4914	4	44097	30248	1.46
GRC	0.44	88	20827	83	3694	15	513	2	4207	1647	2.55
AUT	0.41	54	15658	69	6555	29	323	1	6878	5295	1.30
DNK	0.32	83	6717	72	2355	25	256	3	2611	1590	1.64
LTU	0.30	75	12589	80	2940	19	276	2	3216	2444	1.32
CHE	0.27	64	8218	65	4261	33	254	2	4516	2736	1.65
SVN	0.25	62	4009	72	1557	28	27	0	1583	931	1.70
PRT	0.24	79	14502	69	6124	29	498	2	6622	4367	1.52
EST	0.12	87	8668	84	1613	16	79	1	1692	1133	1.49
LVA	0.07	81	12543	80	3147	20	75	0	3222	2585	1.25
IRL	0.06	80	17473	85	2972	14	78	0	3050	1932	1.58
FIN	0.05	96	65850	87	9889	13	376	0	10265	3953	2.60
SWE	0.04	95	89182	84	16967	16	364	0	17331	8663	2.00
NOR	0.02	95	83390	92	6945	8	219	0	7164	3202	2.24
ISL	0.00	98	40058	97	1060	3	5	0	1065	68	15.7
MLT	0.00	NA	23	100	0	0	0	0	0	0	NA

Table 5
Some example functions that are included in the wOtter source code library.

Functions names	Description and use.
Print_sub_graph	Converts a river graph into a raster with a user-specified attribute from the river graph. This function, for example, was used to create the interactive figure depicting river contamination.
Graph_to_csv	Converts the river network graph into a csv file with a series of selected attributes. This is useful for additional statistical analysis, such as calculating aggregated contamination by basins or countries.
Absorb_shapefile	Extracts attributes from a shapefile and appends these attributes to the river graph. The river node that is located within a polygon from the shapefile receives the value of the selected attribute of the polygon. This function can be used to create a field within the river graph that contains the country or province in which a river cell is located.
Extract_river_network_by_shapefile	Extracts rivers in a region defined by a polygon in a shapefile. An option exists to also include rivers from regions that enter the shapefile. For example, one can extract all rivers in Spain using a polygon for Spain, with the additional option to include rivers that flow into and out of Spain. The output is a graph object.
Find_discharge	Finds the closest river to a raster cell. This is used to link the wastewater discharge points to the closest river section.
Load_selected_attributes_graph	Loads the river graph with a selection of attributes. While this function takes longer than loading all the attributes, speed of subsequent simulation is greatly increased. This function is used in the calibration.

4.3. Implications

The accuracy of MFT models in predicting contamination levels is of great importance, particularly in light of recent proposed EU regulations aimed at reducing concentrations of toxic and persistent chemicals in surface water and groundwater (European Commission, 2022). Current knowledge on the spatial distribution of microcontaminants is based on monitoring programs implemented independently by each EU country, with limited coordination on sampling and analysis. MFT models such as wOtter can help fill gaps in observations to better understand spatial variation in wastewater-derived contamination in water bodies. Such models can locate hot spots of contamination and direct sampling efforts, as well as simulate counterfactuals such as the impact of upgrades to wastewater treatment facilities.

We intend to use wOtter in future work to optimize investment in wastewater treatment given limits on contamination in river bodies. wOtter will also be used to evaluate the influence of climate change on WWTP upgrades (as in Abily et al. (2021) but now including river attenuation). Additionally, we plan to use wOtter to determine the sources of contamination and price them according to cost-sharing algorithms.

4.4. Limitations

When there existed a trade-off between consistency with theory and simplification to improve predictive power, we prioritized simplification. This is most evident in the process of attenuation in water bodies. Microcontaminants attenuation in water bodies is relevant and should be included in MFT models (Acuña et al., 2015b; Aymerich et al., 2016). We only applied first-order attenuation, even when simulating the lumped contaminant despite consisting of multiple compounds with different rates. We believe first-order attenuation is a reasonable simplification, but some studies add more complexity. For example, GREAT-ER considers sedimentation, volatilization, photolysis, hydrolysis, and biodegradation (Kehrein et al., 2015). Jones et al. (2022) adds temperature as a parameter to the attenuation process.

The implementation of wOtter for Europe yielded a large goodness of fit, but there are several limitations to the conclusions of the model. The first limitation is that the model does not predict toxicity but rather an index of toxicity. This means that although we may say that one basin is in a worse state than another, we cannot say that the ecological state is bad. We could attempt to predict toxic units instead of an index, but this would result in a worse proxy for toxicity (see, S6). In addition, quantification of toxicity is difficult due to interactions between contaminants and a simple sum of toxic units may not give a good indication of the ecological state (Varaksin et al., 2014).

The second limitation is that we only considered microcontaminants from households, not other types of contamination. Contamination from industry, farming or illegal dumping may affect water bodies more than micro contamination. For example, a mass death of fish in the river Oder was attributed to salinity caused by industrial pollution (Schulte et al., 2022). In addition, eutrophication due to nitrogen and phosphorus may also adversely affect river ecosystems. Hence microcontaminants are only one aspect of contamination of waterbodies.

The third limitation is that wOtter may not be as accurate for smaller basins. The challenges posed to modeling European rivers by anthropogenic changes in river networks (e.g. artificial diversions of water, canals, etc.) limit the preciseness of our implementation for Europe. For example, the heavily urbanized river and canal network in Utrecht was unsuitable for analysis because residence times, water flow directions and discharges could not be estimated accurately. When using wOtter for a specific basin, we recommend cross-validating the location of WWTPs and contaminants discharge points to water bodies as wOtter does not function properly in some specific areas.

5. Conclusions

wOtter is an open-source, rapid and user-friendly MFT model that can be used to predict wastewater-derived contamination in European river networks. A full simulation of the model requires 25 s, although faster times are possible using different simulation methods. With the speed of implementation, the model is suited for the application of algorithms that require many simulations, such as calibrations, optimization algorithms or Monte-Carlo methods. The model calibration attained an R^2 of 77.5% when using simulation quantities to predict occurrences of a lumped contaminant. This suggests that wOtter and other MFT models can predict spatial variation in wastewater contamination accurately. As such, wOtter may be used in conjunction with sampling efforts to tackle micro contamination of water bodies.

Software availability

Name: wOtter.
Contact: Lluís Corominas at lcorominas@icra.cat.
Year First Available: 2023.
Hardware required: 8 GB ram (16 GB recommended), 60 GB free memory for inputs and outputs used in this study.
Program language: Python.
Program available at: https://github.com/icra/wOtter; manual available in SI.

Funding sources

ICRA authors acknowledge the funding provided by the Spanish Ministry of Science, Innovation and Universities (MICIU), the Agencia Estatal de Investigación (AEI) and the EU FEDER program (project INVEST: RTI2018- 097471-B-C21), the Generalitat de Catalunya through the Consolidated Research Group grant ICRA-Tech 2021-SGR-01283 and ICRA-ENV 2021-SGR-01282, and the funding from the CERCA program of the Catalan Government.

CRediT authorship contribution statement

Janick Klink: Conceptualization, Data curation, Formal analysis, Investigation, Methodology, Software, Writing – original draft, Writing – review & editing. **Laura Aixalà Perelló:** Conceptualization, Formal analysis, Methodology, Software, Visualization. **Morgan Abily:** Conceptualization, Formal analysis, Methodology, Supervision, Writing – review & editing. **Joan Saló:** Software, Visualization. **Ignasi Rodríguez-Roda:** Conceptualization, Funding acquisition, Supervision, Writing – review & editing. **Rafael Marcé:** Conceptualization, Methodology, Software, Validation, Writing – review & editing. **Wolfgang Gernjak:** Conceptualization, Funding acquisition, Methodology, Project administration, Resources, Supervision, Validation, Writing – review & editing. **Lluís Corominas:** Conceptualization, Funding acquisition, Investigation, Methodology, Resources, Supervision, Writing – original draft, Writing – review & editing.

Declaration of competing interest

The authors declare that they have no known competing financial interests or personal relationships that could have appeared to influence the work reported in this paper.

Data availability

Data will be made available on request.

Acknowledgements

We thank Dr. Vicenç Acuña and Prof Manel Poch for their feedback on the manuscript, and Lluís Maria Bosch from ICRA for his contribution to the curation of the UWWTD database. Open Access funding provided thanks to the CRUE-CSIC agreement with Elsevier.

Appendix A. Supplementary data

Supplementary data to this article, including a manual with model details, can be found online at https://doi.org/10.1016/j.envsoft.2024.106049.

References

Abily, M., Acuña, V., Gernjak, W., Rodriguez-Roda, I., Poch-Espallargas, M., Corominas, L., 2022. Assessment of Spanish rivers current and future ecological status using urban wastewater dilution factor. Advances in Hydroinformatics: Models for Complex and Global Water Issues—Practices and Expectations 1087–1101. https://doi.org/10.1007/978-981-19-1600-7_69.

Abily, M., Vicenç, A., Gernjak, W., Rodríguez-Roda, I., Poch, M., Corominas, L., 2021. Climate change impact on EU rivers' dilution capacity and ecological status. Water Res. 199, 117166 https://doi.org/10.1016/J.WATRES.2021.117166.

Acuña, V., Bregoli, F., Font, C., Barceló, D., Corominas, Ll., Ginebreda, A., Petrovic, M, Rodríguez-Roda, I., Sabater, S., Marcé, R., 2020. Management actions to mitigate the occurrence of pharmaceuticals in river networks in a global change context. Environ. Int. 143, 105993. https://doi.org/10.1016/j.envint.2020.105993.

Acuña, V., Ginebreda, A., Mor, J.R., Petrovic, M., Sabater, S., Sumpter, J., Barceló, D., 2015a. Balancing the health benefits and environmental risks of pharmaceuticals: diclofenac as an example. Environ. Int. 85, 327–333. https://doi.org/10.1016/j.envint.2015.09.023.

Acuña, V., von Schiller, D., García-Galán, M.J., Rodríguez-Mozaz, S., Corominas, L., Petrovic, M., Poch, M., Barceló, D., Sabater, S., 2015b. Occurrence and in-stream attenuation of wastewater-derived pharmaceuticals in Iberian rivers. Sci. Total Environ. 503–504, 133–141. https://doi.org/10.1016/J.SCITOTENV.2014.05.067.

Alcamo, J., Döll, P., Henrichs, T., Kaspar, F., Lehner, B., Rösch, T., Siebert, S., 2003. Development and testing of the WaterGAP 2 global model of water use and availability. Hydrol. Sci. J. 48 (3), 317–337. https://doi.org/10.1623/hysj.48.3.317.45290.

Aldred, J., 2011. Banned Livestock Drug Continues to Threaten India's Vultures, Conservatives Warn. Guardian. https://www.theguardian.com/environment/2011/sep/06/diclofenac-india-cattle-vultures.

Allen, P.M., Arnold, J.C., Byars, B.W., 1994. Downstream channel geometry for use in planning-level models. J. Am. Water Resour. Assoc. 30, 663–671. https://doi.org/10.1111/j.1752-1688.1994.tb03321.x.

An Act to Amend the Federal Water Pollution Control Act, Pub. L. No. S.2770, 1971.

Anderson, P.D., D'Aco, V.J., Shanahan, P., Chapra, S.C., Buzby, M.E., Cunningham, V.L., Duplessie, B.M., Hayes, E.P., Mastrocco, F.J., Parke, N.J., Rader, J.C., Samuelian, J. H., Schwab, B.W., 2004. Screening analysis of human pharmaceutical compounds in U.S. Surface waters. Environ. Sci. Technol. 38 (3), 838–849. https://doi.org/10.1021/es034430b.

Aymerich, I., Acuña, V., Barceló, D., García, M.J., Petrovic, M., Poch, M., Rodriguez-Mozaz, S., Rodríguez-Roda, I., Sabater, S., von Schiller, D., Corominas, L., 2016. Attenuation of pharmaceuticals and their transformation products in a wastewater treatment plant and its receiving river ecosystem. Water Res. 100, 126–136. https://doi.org/10.1016/j.watres.2016.04.022.

Buerge, I.J., Kahle, M., Buser, H.R., Müller, M.D., Poiger, T., 2008. Nicotine derivatives in wastewater and surface waters: application as chemical markers for domestic wastewater. Environ. Sci. Technol. 42 (17), 6354–6360. https://doi.org/10.1021/es800455q.

Buerge, I.J., Poiger, T., Müller, M.D., Buser, H.-R., 2003. Caffeine, an anthropogenic marker for wastewater contamination of surface waters. Environ. Sci. Technol. 37 (4), 691–700. https://doi.org/10.1021/es020125z.

Chan, A.Y.L., Yuen, A.S.C., Tsai, D.H.T., Lau, W.C.Y., Jani, Y.H., Hsia, Y., Osborn, D.P.J., Hayes, J.F., Besag, F.M.C., Lai, E.C.C., Wei, L., Taxis, K., Wong, I.C.K., Man, K.K.C., 2023. Gabapentinoid consumption in 65 countries and regions from 2008 to 2018: a longitudinal trend study. Nat. Commun. 14 (1), 5005. https://doi.org/10.1038/s41467-023-40637-8.

Corominas, L., Byrne, D.M., Guest, J.S., Hospido, A., Roux, P., Shaw, A., Short, M.D., 2020. The application of life cycle assessment (LCA) to wastewater treatment: a best practice guide and critical review. Water Res. 184, 116058 https://doi.org/10.1016/j.watres.2020.116058.

Corominas, L., Gimeno, P., Constantino, C., Daldorph, P., Comas, J., 2021. Can source control of pharmaceuticals decrease the investment needs in urban wastewater infrastructure? J. Hazard Mater. 407, 124375 https://doi.org/10.1016/j.jhazmat.2020.124375.

Cunningham, V.L., D'aco, V.J., Pfeiffer, D., Anderson, P.D., Buzby, M.E., Jahnke, J., Hannah, R.E., Parke, N.J., 2012. Predicting concentrations of trace organic compounds in municipal wastewater treatment plant sludge and biosolids using the phate tm model. Integrated Environ. Assess. Manag. 8 (3), 530–542. https://doi.org/10.1002/ieam.1274.

Diener, H.-C., Schneider, R., Aicher, B., 2008. Per-capita consumption of analgesics: a nine-country survey over 20 years. J. Headache Pain 9 (4), 225–231. https://doi.org/10.1007/s10194-008-0046-6.

Duarte, D.J., Niebaum, G., Lämmchen, V., van Heijnsbergen, E., Oldenkamp, R., Hernández-Leal, L., Schmitt, H., Ragas, A.M.J., Klasmeier, J., 2022. Ecological risk assessment of pharmaceuticals in the transboundary vecht river (Germany and The Netherlands). Environ. Toxicol. Chem. 41 (3), 648–662. https://doi.org/10.1002/ETC.5062.

Ehalt MacEdo, H., Lehner, B., Nicell, J., Grill, G., Li, J., Limtong, A., Shakya, R., 2022. Distribution and characteristics of wastewater treatment plants within the global river network. Earth Syst. Sci. Data 14 (2), 559–577. https://doi.org/10.5194/ESSD-14-559-2022.

esamur, 2022. Reutilización. Retrieved February 16, 2023, from. https://www.esamur.com/reutilizacion.

European Commission, 2022. European Green Deal: Commission Proposes Rules for Cleaner Air and Water. Press release office. https://ec.europa.eu/commission/presscorner/detail/en/ip_22_6278.

European Parliament, & European Council, 2000. Directive 2000/60/EC of the European Parliament and of the Council of 23 October 2000 establishing a framework for Community action in the field of water policy. Official Journal of the European Communities 43, 1–73.

Font, C., Bregoli, F., Acuna, V., Sabater, S., Marcé, R., 2019. GLOBAL-FATE (version 1.0.0): a geographical information system (GIS)-based model for assessing contaminants fate in the global river network. Geosci. Model Dev. (GMD) 12 (12), 5213–5228. https://doi.org/10.5194/gmd-12-5213-2019.

Gimeno, P., Marcé, R., Bosch, L., Comas, J., Corominas, L., 2017. Incorporating model uncertainty into the evaluation of interventions to reduce microcontaminant loads in rivers. Water Res. 124, 415–424. https://doi.org/10.1016/J.WATRES.2017.07.036.

Grill, G., Li, J., Khan, U., Zhong, Y., Lehner, B., Nicell, J., Ariwi, J., 2018. Estimating the eco-toxicological risk of estrogens in China's rivers using a high-resolution contaminant fate model. Water Res. 145, 707–720. https://doi.org/10.1016/j.watres.2018.08.053.

Hoffman, S.J., Mammone, J., Katwyk, S. R. Van, Sritharan, L., Tran, M., Al-Khateeb, S., Grjibovski, A., Gunn, E., Kamali-Anaraki, S., Li, B., Mahendren, M., Mansoor, Y., Natt, N., Nwokoro, E., Randhawa, H., Song, M.Y., Vercammen, K., Wang, C., Woo, J., Poirier, M.J.P., 2019. Cigarette consumption estimates for 71 countries from 1970 to 2015: systematic collection of comparable data to facilitate quasi-experimental evaluations of national and global tobacco control interventions. BMJ 365. https://doi.org/10.1136/bmj.l2231.

Jones, E.R., Bierkens, M.F.P., Wanders, N., Sutanudjaja, E.H., van Beek, L.P.H., van Vliet, M.T.H., 2022. Current wastewater treatment targets are insufficient to protect surface water quality. Communications Earth & Environment 3 (1), 1–8. https://doi.org/10.1038/s43247-022-00554-y, 2022 3:1.

Kahle, M., Buerge, I.J., Müller, M.D., Poiger, T., 2009. Hydrophilic anthropogenic markers for quantification of wastewater contamination in ground-and surface WATERS. Environ. Toxicol. Chem. 28 (12), 2528–2536. https://doi.org/10.1897/08-606.1.

Kapo, K.E., DeLeo, P.C., Vamshi, R., Holmes, C.M., Ferrer, D., Dyer, S.D., Wang, X., White-Hull, C., 2016. iSTREEM(®) : an approach for broad-scale in-stream exposure assessment of "down-the-drain" chemicals. Integrated Environ. Assess. Manag. 12 (4), 782–792. https://doi.org/10.1002/ieam.1793.

Kehrein, N., Berlekamp, J., Klasmeier, J., 2015. Modeling the fate of down-the-drain chemicals in whole watersheds: new version of the GREAT-ER software. Environ. Model. Software 64, 1–8. https://doi.org/10.1016/J.ENVSOFT.2014.10.018.

Koormann, F., Rominger, J., Schowanek, D., Wagner, J.O., Schröder, R., Wind, T., Silvani, M., Whelan, M.J., 2006. Modeling the fate of down-the-drain chemicals in rivers: an improved software for GREAT-ER. Environ. Model. Software 21 (7), 925–936. https://doi.org/10.1016/j.envsoft.2005.04.009.

Lämmchen, V., Klasmeier, J., Hernandez-Leal, L., Berlekamp, J., 2021. Spatial modelling of micro-pollutants in a strongly regulated cross-border lowland catchment. Environmental Processes 8 (3), 973–992. https://doi.org/10.1007/s40710-021-00530-2.

Lehner, B., Verdin, K., Jarvis, A., 2008. New global hydrography derived from spaceborne elevation data. Eos, Transactions American Geophysical Union 89 (10), 93–94.

Pistocchi, A., Alygizakis, N.A., Brack, W., Boxall, A., Cousins, I.T., Drewes, J.E., Finckh, S., Gallé, T., Launay, M.A., McLachlan, M.S., Petrovic, M., Schulze, T., Slobodnik, J., Ternes, T., van Wezel, A., Verlicchi, P., Whalley, C., 2022. European scale assessment of the potential of ozonation and activated carbon treatment to reduce micropollutant emissions with wastewater. Sci. Total Environ. 848, 157124 https://doi.org/10.1016/J.SCITOTENV.2022.157124.

Pistocchi, A., Sarigiannis, D.A., Vizcaino, P., 2010. Spatially explicit multimedia fate models for pollutants in Europe: state of the art and perspectives. Sci. Total Environ. 408 (18), 3817–3830. https://doi.org/10.1016/j.scitotenv.2009.10.046.

Reyes, C., Cornelis, M., 2018. Caffeine in the diet: country-level consumption and guidelines. Nutrients 10, 1772. https://doi.org/10.3390/nu10111772.

Rice, J., Westerhoff, P., 2015. Spatial and temporal variation in de facto wastewater reuse in drinking water systems across the U.S.A. Environ. Sci. Technol. 49 (2), 982–989. https://doi.org/10.1021/ES5048057/SUPPL_FILE/ES5048057_SI_001.PDF.

Schulte, C., Abbas, B., Engelke, C., Fischer, H., Henneberg, S., Hentschel, H., Jekel, H., Jeske, R., Pietsch, K., Schöll, F., Schönfelder, J., Ternes, T., Völker, J., 2022. Fish die-off in the oder river, august 2022. https://www.bmuv.de/en/download/status-report-on-fish-die-off-in-the-oder-river.

Schulze, K., Hunger, M., Döll, P., 2005. Simulating river flow velocity on global scale. Adv. Geosci. 5, 133–136.

Schwarzenbach, R.P., Escher, B.I., Fenner, K., Hofstetter, T.B., Johnson, C.A., von Gunten, U., Wehrli, B., 2006. The challenge of micropollutants in aquatic systems. Science 313 (5790), 1072–1077. https://doi.org/10.1126/SCIENCE.1127291.

Varaksin, A.N., Katsnelson, B.A., Panov, V.G., Privalova, L.I., Kireyeva, E.P., Valamina, I. E., Beresneva, O.Y., 2014. Some considerations concerning the theory of combined toxicity: a case study of subchronic experimental intoxication with cadmium and lead. Food Chem. Toxicol. 64, 144–156. https://doi.org/10.1016/j.fct.2013.11.024.

Verlicchi, P., Al Aukidy, M., Zambello, E., 2012. Occurrence of pharmaceutical compounds in urban wastewater: removal, mass load and environmental risk after a secondary treatment-A review. Sci. Total Environ. 429, 123–155. https://doi.org/10.1016/j.scitotenv.2012.04.028.

Vigiak, O., Grizzetti, B., Zanni, M., Aloe, A., Dorati, C., Bouraoui, F., Pistocchi, A., 2020. Domestic waste emissions to European waters in the 2010s. Sci. Data 7 (1), 1–13. https://doi.org/10.1038/s41597-020-0367-0, 2020 7:1.

Virtanen, P., Gommers, R., Oliphant, T.E., Haberland, M., Reddy, T., Cournapeau, D., Burovski, E., Peterson, P., Weckesser, W., Bright, J., van der Walt, S.J., Brett, M., Wilson, J., Millman, K.J., Mayorov, N., Nelson, A.R.J., Jones, E., Kern, R., Larson, E., et al., 2020. SciPy 1.0: fundamental algorithms for scientific computing in Python. Nat. Methods 17 (3), 261–272. https://doi.org/10.1038/s41592-019-0686-2.

Whalley, C., Busch, W., van den Roovaart, J., van Dujnhoven, N., Kirst, I., Schmedtje, U., Altenburger, R., Sommer, L., 2018. Chemicals in European waters : knowledge developments. https://www.eea.europa.eu/publications/chemicals-in-european-waters.

Wilkinson, J.L., Boxall, A.B.A., Kolpin, D.W., Leung, K.M.Y., Lai, R.W.S., Galban-Malag, C., Adell, A.D., Mondon, J., Metian, M., Marchant, R.A., Bouzas-Monroy, A., Cuni-Sanchez, A., Coors, A., Carriquiriborde, P., Rojo, M., Gordon, C., Cara, M., Moermond, M., Luarte, T., et al., 2022. Pharmaceutical pollution of the world's rivers. Proc. Natl. Acad. Sci. U.S.A. 119 (8), e2113947119 https://doi.org/10.1073/PNAS.2113947119/SUPPL_FILE/PNAS.2113947119.SD12.XLSX.

Young, A.R., Grew, R., Holmes, M.G.R., 2003. Low Flows 2000: a national water resources assessment and decision support tool. Water Sci. Technol. 48 (10), 119–126. https://doi.org/10.2166/wst.2003.0554.